Food Chemistry 400 (2023) 134110

Contents lists available at ScienceDirect

Food Chemistry

journal homepage: www.elsevier.com/locate/foodchem

Effect of the addition of soluble polysaccharides from red and white grape skins on the polyphenolic composition and sensory properties of Tempranillo red wines

Elvira Manjón [a,1], Siyu Li [a,b,1], Montserrat Dueñas [a], Ignacio García-Estévez [a,*], María Teresa Escribano-Bailón [a]

[a] Grupo de Investigación en Polifenoles, Facultad de Farmacia, Universidad de Salamanca, Salamanca E37007, Spain
[b] Institute for Horticultural Plants, College of Horticulture, China Agricultural University, Beijing 100083, China

ARTICLE INFO

Keywords:
Wine
Flavan-3-ols
Anthocyanins
Astringency
Color
Climate change

ABSTRACT

Soluble polysaccharides from white (PSW) and red (PSR) grape skins were obtained to be evaluated as potential modulators of the unbalanced astringency of a Tempranillo red wine. The modulation of astringency was evaluated by a sensory panel and it seemed to be related to the changes in the polyphenolic profile. Isothermal Titration Calorimetry (ITC) studies, employed to characterize flavan-3-ol–polysaccharide interactions, showed that PSR decreased noticeably wine astringency causing a great flavan-3-ol loss (*ca.* 40 %), since they interacted more spontaneously with the flavan-3-ols (*ca.* ΔGtotal = -2.14×10^4 cal/mol) than PSW (*ca.* ΔGtotal = -1.32×10^4 cal/mol). The strength of these interactions seems to be related to the polysaccharide molecular size and to the presence of arabinogalactans in the structure. On the contrary, PSW showed no relevant effects on wine astringency. Furthermore, potential variations of color were also assessed and no deleterious effect was observed after the addition of any polysaccharide.

1. Introduction

Polyphenols, including flavan-3-ols, anthocyanins and flavonols, are secondary metabolites synthesized in grapes that play important roles affecting wine astringency and color (Ferrer-Gallego et al., 2015; Soares et al., 2019; Ferrer-Gallego et al., 2016; Scollary, Pásti, Kállay, Blackman, & Clark, 2012). Technological maturity of the grape (sugar content, titratable acidity and pH of the grape juice) is traditionally used for determining the harvest date. Besides, optimum quantitative and qualitative profile of polyphenols in grapes (phenolic maturity) are considered by enologists as key parameters to evaluate grape quality at harvest. Due to the influence of global climate change, the delay between these two types of maturity has increased –the technological maturity is increasingly early while the phenolic one is increasingly late– which leads to an increase in flavan-3-ols and a decrease of coloring matter stability in wines (becoming too astringent and with poor color)(Jones, White, Cooper, & Storchmann, 2005). To solve this problem, several strategies have been proposed, among them, the addition of

Abbreviations: **AG**, Arabinogalactan; **AMO**, Acylated monoglucosides; **ARA**, Arabinan; **Ara**, Arabinose; **C**, Control; **CWM**, Cell Wall Material; **DPC**, Dimeric Procyanidins; **DPD**, Dimeric Prodelphinidins; **EMS**, Enhance Mass Spectrometry; ***EPI***, Enhance Product Ion; **F**, Flavan-3-ol extract from grape seeds; **FA**, Flavan-3-ol-anthocyanin direct condensation products; **FeA**, Flavan-3-ol-anthocyanin acetaldehyde-mediated condensation products; **GMF**, Galloylated Monomeric Flavan-3-ols; **HG**, Homogalacturonan; ***K***, Apparent binding constant; **LMS**, Labeled Magnitude Scale; **MAN**, Mannan; **Man**, Mannose; **MRM**, Multiple Reaction Monitoring; **MW**, Molecular Weight; **mMW**, Medium Molecular Weight; **NAMO**, Non-acylated monoglucosides; **NGMF**, Non-Galloylated Monomeric Flavan-3-ols; **OM**, Procyanidin-prodelphinidin mixed oligomers; **OPC**, Oligomeric Procyanidins; **PMP**, 1-phenyl-3-methyl-5-pyrazolone; **PSR**, Soluble Polysaccharides from Red grape skins; **PSW**, Soluble Polysaccharides from White grape skins; **RG I**, Rhamnogalacturonan I; **RG II**, Rhamnogalacturonan II; **VitA**, A-type vitisins; **VitB**, B-type vitisins; **VitVF**, Vinylphenol-type pyranoanthocyanins; **XG**, Xyloglucan; **1W**, One-week; **2M**, Two-months; **3W**, Three-weeks; **Δ*G***, Changes in Gibbs free energy; **ΔE^*_{ab}**, Changes in color differences; **Δ*H***, Changes in enthalpy; **Δ*S***, Changes in entropy; **%Δ^{2}C**, Quadratic differences of Chroma; **%Δ^{2}H**, Quadratic differences of Hue; **%Δ^{2}L**, Quadratic differences of Lightness.

* Corresponding author.
E-mail address: igarest@usal.es (I. García-Estévez).
[1] Both authors contributed equally to this manuscript.

https://doi.org/10.1016/j.foodchem.2022.134110
Received 30 March 2022; Received in revised form 8 August 2022; Accepted 1 September 2022
Available online 6 September 2022

insoluble polysaccharides from grape skin cell walls, based mainly on the retention of tannins in the insoluble cell wall material (Jiménez-Martínez, Bautista-Ortín, Gil-Muñoz, & Gómez-Plaza, 2019; Guerrero, Smith, & Bindon, 2013).

Grape skin cell walls are usually composed of structural proteins (~10 %) and polysaccharides (~90 %), the latter are grouped into three categories: cellulose, hemicellulose and pectin (Zhang, Gao, Zhang, & Zhou, 2021). Polysaccharides can interact with phenolic compounds through hydrophobic interactions and hydrogen bonds due to their hydroxyl groups and aromatic and glycosidic oxygen atoms (Le Bourvellec & Renard, 2012) being able to decrease the extractability of tannins presumably by their retention in grapes during winemaking (Bautista-Ortín, Martínez-Hernández, Ruiz-García, Gil-Muñoz, & Gómez-Plaza, 2016) or reducing tannin content by adsorption once cell wall material (CWM) is suspended in grape musts or wines (Jiménez-Martínez et al., 2019; Guerrero et al., 2013).

So far, most authors that have investigated the role of grape CWM on wine polyphenolic composition and sensory properties have employed insoluble CWM. The use of insoluble CWM could decrease wine astringency both because the polysaccharides in CWM could bind flavan-3-ols and because the special porous structure of CWM would benefit flavan-3-ol absorption (Bindon, Smith, & Kennedy, 2010). However, there are still several disadvantages for insoluble CWM: first, interactions between CWM and flavan-3-ols are greatly dependent on the composition of grape skin since high content in cellulose and lignin are positively correlated with cell wall rigidity, which may perturb the binding affinity for flavan-3-ols (Jiménez-Martínez, Bautista-Ortín, Gil-Muñoz, & Gómez-Plaza, 2019; Bindon, Bacic, & Kennedy, 2012); second, the addition of insoluble fibers into wines can caused anthocyanin and color intensity loss (Jiménez-Martínez et al., 2019; Guerrero et al., 2013; Jiménez-Martínez et al., 2019).

Given the disadvantages of the insoluble CWM, the hypothesis of this study is that soluble CWM from grape skins may be a new alternative in modulating harsh or unbalanced astringency in wines. The purpose of this work was to obtain different soluble polysaccharide materials from red and white grape skins and to evaluate, for the first time, their ability to interact with flavan-3-ols and to modulate wine astringency. Furthermore, because every action exerted on astringency must be evaluated in terms of color, the effect of soluble CWM directly on color parameters and on the phenolic composition of Tempranillo red wine has also been assessed.

2. Materials and methods

2.1. Chemicals

All reagents used were of analytical grade (purity > 95 %), and all solvents were of HPLC grade (purity > 98 %). Pullulan Standard Set and 1-phenyl-3-methyl-5-pyrazolone (PMP) were acquired from Sigma-Aldrich (St. Louis, MO). 2-Deoxy-D-ribose and chlorogenic acid were purchased from Alfa-Aesar, (Karlsruhe, Germany). Malvidin 3-*O*-glucoside was obtained from Extrasynthèse (Genay, France). Ethanol was purchased from Scharlab S.L. (Barcelona, Spain). H_2SO_4, HCl and acetic acid were acquired from Panreac (Darmstadt, Germany). Acetonitrile was acquired from Supelco (Darmstadt, Germany), formic acid from VWR Prolabo (France) and trifluoroacetic acid from Riedel-de Haën (Hanover, Germany). Ultrapure water was obtained from a Milli-Q Gradient water purification system (Millipore, Billerica, MA).

2.2. Grape seed Flavan-3-ol extract

Vitis vinifera L. Tempranillo grapes were collected at veraison, since they have an unbalanced flavan-3-ol composition similar to that showed by grapes growth under a climate change scenario. Seeds were separated from the skins and pulp, then frozen at −20 °C for 24 h, freeze-dried in a Telstar LyoQuest system (Barcelona, Spain) and grounded in a CH-6014 Littau-Lu (Kinematica AG, Switzerland) to obtain a homogeneous powder. Grape seed flavan-3-ol extract was obtained following the procedure previously described (Alcalde-Eon, Ferreras-Charro, et al., 2019). Briefly, the resulting powder was extracted 3 times with ethanol/water (75:25, *v/v*) for 30 min at an output power of 11 W in an ultrasonic bath (Microson ultrasonic cell disruptor XL, Misonix Inc., Farmingdale, NY, USA). The solution was then centrifuged (10 min at 16,500 g), and the supernatant was evaporated in a rotavapor R-210 (Buchi, Switzerland) to remove the organic solvent. The aqueous grape seed flavan-3-ol extract was frozen and freeze-dried, and stored at 4 °C until use. Detailed flavan-3-ol composition was analyzed following the method described by García-Estévez and coworkers (García-Estévez, Alcalde-Eon, & Escribano-Bailón, 2017) and provided in Supplementary Material (Table S1).

2.3. Isolation of soluble grape skin cell wall Material

White (*V. vinifera* L. Muscat) and red (*V. vinifera* L. Tempranillo) grapes were collected at technological maturity (20.2 °Brix and total acidity 6.1 g/L (eq. tartaric acid) and 23.1 °Brix and total acidity 4.9 g/L (eq. tartaric acid), respectively) and their skins were manually separated. White grapes were collected from Monforte del Cid (Spain) and red grapes from La Horra (Spain). Each type of grape skins was extracted in boiling water for 2 h (30 g grape skins per liter) for polysaccharide extraction based on the procedure described by Martins and coworkers (Martins et al., 2017). Afterwards, supernatants were concentrated under reduced pressure and added with ethanol to reach a final concentration of 30 % (*v/v*) in order to precipitate less soluble cell wall material (CWM). The solutions were kept at 4 °C for 2 h and the precipitates obtained were discarded by centrifugation (9,500 g for 10 min at 4 °C). Ethanol was evaporated and the solutions were dialyzed for 2 days to remove small molecules using a dialysis membrane with an exclusion size of 12–14 kDa (Medicell International ltd., London, UK). Then, soluble CWM was precipitated by adding 75 % *v/v* ethanol (Martins et al., 2017). Mixtures were kept at 4 °C for 2 h and centrifuged at 9,500 g for 20 min at 4 °C. The precipitates were collected and washed with 96 % ethanol until the ethanolic supernatants were colorless. The precipitates were then submitted to a solid-phase extraction using C18 columns for CWM purification by eluting CWM with water. The resulting soluble CWM –namely soluble CWM from the first extraction– was frozen at −20 °C for 24 h and then it was freeze-dried (yield *ca.* 2 %). Simultaneously, the grape skins already extracted were again collected and subjected to the isolation process described above, in order to obtain the soluble CWM from the second extraction (yield *ca.* 1 %).

2.4. Samples and experimental design

A commercial red wine (13.5° alcohol (*v/v*) and pH 3.54) was selected as reported in Manjón et al. (Manjón, Brás, García-Estévez, & Escribano-Bailón, 2020) and the obtained grape seed flavan-3-ol extract was added to it (c = 750 mg/L) in order to increase its astringency. 24 h after the addition of the seed extract, the wine was divided into five batches. One of them was used as a control wine (C-wine) and the other four (PSW1-wine; PSW2-wine; PSR1-wine and PSR2-wine) were supplemented with soluble CWM (50 mg/L) from white grapes of first extraction (PSW1), from white grapes of second extraction (PSW2), from red grapes of first extraction (PSR1) or from red grapes of second extraction (PSR2), respectively. All samples were conducted in triplicate in black glass bottles of 250 mL and analyzed (flavan-3-ols, anthocyanins, astringency, color) after one-week (1 W), three-weeks (3 W) and two-months (2 M) of storage at 22 °C.

2.5. Grape skin Macromolecule analysis

The molecular weight (MW) distribution of each macromolecule fraction was determined by high-performance size exclusion

chromatography on an Agilent 1260 Infinity HPLC system (Agilent Technologies, Palo Alto, CA) equipped with a refractive index detector (RID), using two serial Shodex OHpak SB-803 HQ and SB-804 HQ columns (300 mm × 8 mm) (Showa Denko Europe GmbH, Germany) thermostatted at 60 °C, with a flow rate of 1 mL/min in 0.1 M $LiNO_3$ as previously described (Manjón et al., 2020). For sample preparation, 4 mg of each CWM were dissolved in 1 mL of 0.1 M $LiNO_3$. This solution was filtered through a 0.45 μm Millex syringe-driven filter unit (Millipore Corp., Bedford, MA) and then, 100 μL were injected in the HRSEC-RID system. MWs were calculated from the calibration curve obtained (log MW = 9.9608–0.3821 × t_R, where t_R = retention time at peak maximum, in min) from pullulan molecular weight standards (*P*1, MW = 342 Da; *P*2, MW = 1 320 Da; *P*3, MW = 6 200 Da; *P*4, MW = 10 000 Da; P5, MW = 21 700 Da; *P*6, MW = 48 800 Da; P7, MW = 113 000 Da; P8, MW = 200 000 Da; P9, MW = 348 000 Da; P10, MW = 805 000 Da) by using the Analyst 5.1 software. All analyses were performed in triplicate.

2.6. Analysis of monosaccharide composition

Soluble CWM was hydrolyzed in 12 M H_2SO_4 for 3 h at room temperature, afterward diluted to 1 M H_2SO_4 with Milli-Q water and heated at 100 °C for 2.5 h. Samples were cooled on ice and centrifuged at 140 g for 5 min. In each sample, the supernatant was collected and subjected to derivatization with PMP. The analysis of released monosaccharides was performed following the method of Zhang and co-workers with some modifications (Zhang, Zhang, Wang, & Huang, 2011). Each hydrolyzed extract was neutralized with 10 M ammonium solution. Then, PMP methanol solution (0.05 M) and 2-deoxy-D-ribose as internal standard were added. This mixture was incubated at 60 °C for 50 min to perform the derivatization. After cooling, solutions were neutralized with 3 M HCl and diluted with water to a final volume of 1 mL. The aqueous phase was extracted three times with 1 mL chloroform to eliminate excess PMP and centrifuged (14000 g, 2 min) for subsequent analysis by HPLC-DAD connected to mass spectrometer (MS). The analysis of PMP monosaccharides derivatives was carried out on a Hewlett-Packard-1100 HPLC-DAD chromatograph (Agilent Technologies, Palo Alto, CA) equipped with a quaternary pump and diode array detector (DAD). Separation was performed in an Poroshell 120 EC-C18 (150 mm × 4.6, 2.7 μm, Agilent Technologies) at 25 °C, with a flow rate of 0.5 mL/min. The solvents used were 0.01 M ammonium acetate containing 0.02 % triethylamine adjusted to pH 7.5 with acetic acid (solvent A) and 100 % acetonitrile (solvent B). The elution gradient established was: isocratic 15 % B for 20 min, 25–40 % B for 15 min, 40–90 % B for 5 min, and re-equilibration of the column for 10 min. DAD was carried out using 250 nm as preferred wavelength.

MS was connected to the HPLC system via the DAD cell outlet. MS detection and quantification of monosaccharide derivatives was performed by using a 3200 Qtrap (Applied Biosystems, Darmstadt, Germany) equipped with an ESI source, triple quadrupole-ion trap mass analyzer and controlled by the Analyst 5.1 software. Nebulized gas (20 psi) and turbo gas (400 °C, 40 psi) used for solvent drying were zero grade air, whereas nitrogen served as curtain (20 psi) and collision gas (medium). Both quadrupoles were set up as unit resolution and the ion spray voltage was set up as 4500 V in the positive-ion mode. Multiple reaction monitoring analysis (MRM mode) was employed to detect the transitions (each precursor ion-product ion pair) corresponding to derivatized monosaccharides and including also the derivatized internal standard (2-deoxy-D-ribose). Settings used were as follows: declustering potential (DP) was 80 or 90 V; entrance potential (EP), 6 or 8 V; and collision energy (CE) was 31, 33 or 35 eV depending on the monitored transition. For the calculation of polysaccharide profile, the content of each polysaccharide family was estimated using the iterative from monosaccharide profiles according to Arnous & Meyer (Arnous & Meyer, 2009). All analyses were performed in triplicate.

2.7. Flavan-3-ol analysis

HPLC-MS was used to identify and quantify flavan-3-ols according to previously published method (García-Estévez et al., 2017). For grape seed flavan-3-ols, samples were first dissolved in ultrapure water. For wine flavan-3-ols, prior to analysis, fractionation was carried out to eliminate anthocyanins (Alcalde-Eon, García-Estévez, Ferreras-Charro, et al., 2014). Briefly, wine samples were diluted 1:1 with acidified water (0.1 M HCl), then loaded on an Oasis MCX cartridge (Waters Corp., Milford, MA, USA) previously conditioned with 2 mL of methanol and 2 mL of water. After washing with water (4 mL), flavan-3-ols were eluted with 8 mL of methanol. The eluate was concentrated under vacuum and re-dissolved in 500 μL of water. Chlorogenic acid was added (0.025 mg/mL) as internal standard and samples were filtered through a 0.45 μm Millex syringe-driven filter unit (Millipore Corp., Bedford, MA) before HPLC-DAD-MS analysis (García-Estévez et al., 2017).

HPLC analysis was performed in a Hewlett-Packard 1200 series liquid chromatograph (Agilent Technologies, Waldbronn, Germany). The stationary phase was a Poroshell 120 EC-C18 column (150 × 4.6 mm *i.d.*, 2.7 μm, Agilent Technologies) thermostatted at 25 °C. The mobile phase was composed of 0.1 % (*v*/*v*) aqueous formic acid solution (solvent A), and HPLC grade acetonitrile (solvent B). The following gradient was used at a flow rate of 0.5 mL/min: 10 % B for 3 min, from 10 to 15.5 % B for 34 min, from 15.5 to 20 % B for 3 min, from 20 to 35 % B for 15 min, from 35 to 60 % B for 5 min, and a final isocratic gradient of 60 % B for 3 min. Spectra were recorded from 220 to 600 nm and detection was carried out at 280 nm as the preferred wavelength. MS detection was performed by using the 3200 Qtrap equipment (Applied Biosystems, Darmstadt, Germany). Detection was carried out in positive-ion mode (ESI^+). Nebulizer gas (30 psi) and turbo gas used for solvent drying (300 °C, 40 psi) were zero grade air, whereas nitrogen served as curtain (20 psi) and collision gas (high). Both quadrupoles were set up as unit resolution, and the ion spray voltage was set up as 5500 V in the positive-ion mode. MRM analysis was employed to detect the transitions (each precursor ion – product ion pair) corresponding to each kind of flavan-3-ol and to the internal standard (chlorogenic acid). Compounds were identified from the data supplied by the HPLC-MS^n analysis of the samples (retention time, *m*/*z* ratio, and fragmentation patterns) and by comparison to data previously obtained in our laboratory for wine samples analyzed in the same conditions (García-Estévez et al., 2017).

2.8. Anthocyanin analysis

Anthocyanins and their derivative pigments in wines were analyzed by HPLC-DAD-MS^n. Wine samples were diluted 1:1 with acidified water (0.1 M HCl) and filtered through a 0.45 μm Millex syringe-driven filter unit (Millipore Corp., Bedford, MA) before HPLC-DAD-MS^n analysis. Analysis was performed in a Hewlett-Packard 1100 series liquid chromatograph (Agilent Technologies, Waldbronn, Germany). An Aqua C18 reversed-phase, 5 μm, 150 mm × 4.6 mm column (Phenomenex, Torrance, CA) thermostatted at 35 °C was used. The HPLC-DAD conditions have been previously employed with satisfactory results in our laboratory in the analysis of other wine samples (Alcalde-Eón, Escribano-Bailón, Santos-Buelga, and Rivas-Gonzalo, 2006). Spectra were recorded from 220 to 600 nm and detection was carried out at 520 nm as the preferred wavelength. MS detection was performed by using the 3200 Qtrap (Applied Biosystems, Darmstadt, Germany). Detection was carried out in positive-ion mode (ESI^+). Nebulizer gas (40 psi) and turbo gas used for solvent drying (300 °C, 50 psi) were zero grade air, whereas nitrogen served as curtain (10 psi) and collision gas (high). Declustering potential was set up as 20 V, entrance potential at 10 V, ion spray voltage at 5000 V, and the temperature of the probe at 600 °C. Both quadrupoles were set up as unit resolution. Three types of mass experiments were performed: a full mass analysis (enhance mass spectrometry (EMS) mode, collision energy 10 eV), where all ions were detected, an MS^2

analysis (enhance product ion (*EPI*) mode, collision energy 30 eV), where the major ion of the full mass analysis was fragmented, and a MS^3 analysis (collision energy 30 eV, excitation energy 80 V), where the major fragment ion of the MS^2 analysis was, in turn, fragmented. Spectra were recorded between *m/z* 150 and 1400.

Compounds were identified from the data supplied by the HPLC-DAD-MS^n analysis of the samples (retention time, UV−vis spectra, *m/z* ratio, and fragmentation patterns) and by comparison to data previously obtained in our laboratory for wine samples analyzed in the same conditions (Alcalde-Eon, García-Estévez, Ferreras-Charro, et al., 2014). Individual and total pigment contents of each sample were calculated by means of a malvidin 3-*O*-glucoside calibration curve.

2.9. Astringency evaluation

Wine astringency (C-wine, PSW1-wine, PSW2-wine, PSR1-wine, PSR2-wine) was evaluated by a sensory panel composed of 8 panelists (3 men and 5 women) aged between 25 and 60 years old, who were trained to recognize and to rate the perceived intensity of astringency as reported in Ferrer-Gallego et al., 2015 (Ferrer-Gallego et al., 2015). Previous to the training, all panelists had to sign an informed consent in order to participate in the sensory studies. Briefly, the panelists agreed to attend four preliminary training sessions focused on the recognition of astringency and to standardize the use of the Labeled Magnitude Scale (LMS). In the first two sessions, the panelists had to identify-two identical samples. For it, they tasted three samples, two of them supplemented with the same amount of seed extract and therefore, with high level of astringency, and one control sample without supplementation that showed balanced level of astringency. The objective of this test (performed twice) was that the panelists were able to identify the two astringent samples and, thus, became familiar with the specific astringent sensation. The intensity of astringency was evaluated in the next blind trials (performed also in duplicate). For these sessions, four wine samples supplemented with known and increasing amounts of flavanol extract and one control wine were prepared. The panelists performed a blind tasting of the samples, and they were asked to mark when they began to feel some astringent stimuli and to rate the samples on ascending order by using the LMS. After training, the panelists were asked to evaluate perceived astringency of the samples and to order their astringency intensity on the LMS. It was analyzed by taking 8 mL of each sample, tasting it during 15 s, and spitting it out, without knowing the nature of the samples, since all samples were always presented randomized in black glass bottles to avoid any bias in the results. Then, the panelists rated the intensity for astringency. This protocol was repeated three times per sample to assign the final value in the LMS. This scale is characterized by a quasilogarithmic spacing of its verbal labels from 0 (“barely detectable” oral sensation) to 100 (“strongest imaginable” oral sensation) Manjón et al., 2020; Ferrer-Gallego et al., 2015; Green et al., 1996).

2.10. Colorimetric measurements

Absorption spectra (190–770 nm) were recorded in a Hewlett-Packard UV−vis HP 8453 (Agilent Technologies, Waldbronn, Germany) spectrophotometer using 2 mm path length quartz cells. The analysis of color was made from the visible spectra (380–770 nm) data, applying the CIE standard illuminant D65 and the CIE 1964 standard observer (10° visual field) as references. CIELAB color parameters (L^*, a^*, b^*, C^*_{ab}, and h_{ab}) were calculated using the software CromaLab (Heredia, Álvarez, González-Miret, & Ramírez, 2004). Color difference (ΔE^*_{ab}) between the control wine and the wine samples added with PSW1, PSW2, PSR1, and PSR2 was calculated as the Euclidean distance between two color points in the CIELAB space (Gordillo et al., 2015; Gordillo, Rodríguez-Pulido, Escudero-Gilete, Gonzalez-Miret, & Heredia, 2012).

2.11. Isothermal Titration Calorimetry (ITC) assays

A MicroCal PEAQ-ITC system (SYS80004) (Malvern, U.K.) was used to measure the heat generated or absorbed upon the interactions between grape seed flavan-3-ols (F) and soluble grape skin cell wall materials (PSW1, PSW2, PSR1, and PSR2) at the constant temperature of 298.15 K. All solutions were prepared in ultrapure water and blank experiment (flavan-3-ol–water) was firstly conducted. For each flavan-3-ol–CWM interaction, the flavan-3-ol solution (750 μM) was loaded into the injection syringe and the CWM solution (25 μM) was placed into the 0.2 mL sample cell of the calorimeter. The syringe solution was titrated into the sample cell as a sequence of 19 injections of 2 μL aliquots with one initial delay (time for equilibration) of 300 s. The content of the sample cell was stirred throughout the experiment at 750 rpm.

The software AFFINIMETER (Software for Science Developments, Santiago de Compostela, Spain) was used for data treatment, thus allowing us to obtain the apparent binding constant (*K*), the change in enthalpy (ΔH), entropy ($-\Delta S$), and Gibbs free energy (ΔG). Fittings were carried out by using an independent sites model with two set of sites (two different types of sites for the interaction), in which blank experiment was subtracted from the corresponding interactions. All experiments were performed in triplicate.

2.12. Statistical analysis

The statistical significance of the differences was assessed by Tukey’s honestly significant difference test ($p < 0.05$) and Principal Component Analysis (PCA) was used to observe relationships between samples and/or between variables at 2 M of storage. The Windows IBM SPSS 23 (SPSS, Inc., Chicago, IL, U.S.A.) was used to perform the statistical analysis.

3. Results and discussion

3.1. Soluble grape skin cell wall material

Four soluble cell wall materials were obtained, two of them from red grape skins (PSR1 and PSR2) and other two from white grape skins (PSW1 and PSW2). Each soluble CWM was characterized: the medium molecular weight (mMW) was calculated by using size exclusion chromatography (HRSEC-RID) and the carbohydrate composition was determined by means of HPLC-DAD-MS. The results showed that the mMW of white grape CWM (PSW1 and PSW2) was ~125 kDa and ~141 kDa, respectively, whereas that from red grapes (PSR1 and PSR2) was

Table 1
Medium Molecular Weight (mMW) and compositional characteristics of CWM from different grape skins.

	White grapes (1st extraction) PSW1	White grapes (2nd extraction) PSW2	Red grapes (1st extraction) PSR1	Red grapes (2nd extraction) PSR2
	mMW (kDa)			
	125 ± 3 ^{d}	141 ± 4^{c}	195 ± 6 ^{a}	165 ± 4^{b}
PS family	Percentage			
HG	44.3 ± 0.6^{c}	62.5 ± 0.8 ^{a}	52 ± 1^{b}	51 ± 1^{b}
RG I	4.36 ± 0.06^{c}	6.16 ± 0.08 ^{a}	5.1 ± 0.1^{b}	5 ± 0.1^{b}
RG II	4.2 ± 0.2 ^{a}	0.57 ± 0.02^{c}	0.68 ± 0.01^{c}	2.26 ± 0.02^{b}
AG	17 ± 3^{c}	15 ± 1^{c}	35.7 ± 0.6 ^{a}	29.3 ± 0.3^{b}
ARA	19 ± 3 ^{a}	13.6 ± 0.3^{b}	2.8 ± 0.5 ^{d}	6.3 ± 0.3^{c}
XG	9 ± 2 ^{a}	2.1 ± 0.7^{c}	3 ± 1^{c}	5.7 ± 1.6^{b}
MAN	2.39 ± 0.02 ^{a}	0.52 ± 0.03 ^{d}	1.10 ± 0.03^{b}	0.98 ± 0.04^{c}

HG: homogalacturonan; RG I: rhamnogalacturonan I; RG II: rhamnogalacturonan II; AG: arabinogalactan; ARA: arabinan; XG: xyloglucan; MAN: mannan. Different letters within the same row indicate significant differences ($p < 0.05$, n = 3).

~195 kDa and ~165 kDa, respectively (Table 1). These data indicate that soluble red grape CWM contained larger molecular-weight macromolecules than soluble white grape CWM.

As for the glycoside composition, the content of each polysaccharide family was estimated by using the iterative calculation from monosaccharide profiles (Arnous & Meyer, 2009) (Table S2 of Supplementary Material). Table 1 shows the detailed compositional analysis for polysaccharides from soluble grape skin CWM, including homogalacturonan (HG), rhamnogalacturonan I (RG I), rhamnogalacturonan II (RG II), arabinogalactan (AG), arabinan (ARA), xyloglucan (XG) and mannan (MAN). In all CWM, HG was the main type of polysaccharides (44.27 ~ 62.54 %) and arabinose-related polysaccharides (AG, calculated from galactose (Gal) and arabinose (Ara) monosaccharides, considering the Gal:Ara ration of 1.5:1 and ARA (calculated from remaining arabinose) were the polysaccharides with the second highest proportion, with noticeable differences depending on the CWM. It is widely acknowledged that HG, AG and ARA polysaccharides are the main components of the pectic network of grape cell walls (Martínez-Lapuente, Guadalupe, & Ayestaran, 2019). Here, red grape CWM (PSR1 and PSR2) presented statistically higher proportions of AG and statistically lower proportions of ARA than their white grape counterparts (PSW1 and PSW2) (Table 1).

Other polysaccharides (RG I, RG II, XG, MAN) were found in proportions lower than 10 % in all CWM samples. Regarding MAN, it is commonly found in grapes in minor proportion than other polysaccharides and it has been postulated that it could derived from yeasts cell wall existing in wax layer of grapes (Guadalupe, Martínez, & Ayestarán, 2010) but its own presence in CWM of grapes cannot be discounted. As for XG, it should be derived from hemicellulose, which may be partly dissolved during extraction (Arnous & Meyer, 2009).

3.2. Analysis of CWM–flavan-3-ol interactions by Isothermal Titration Calorimetry (ITC)

It has been postulated that interactions between tannins and polysaccharides lead to complexes that can help to improve the sensations of body and volume in the mouth and to reduce some tannic astringency (Jones-Moore, Jelley, Marangon, & Fedrizzi, 2022; García-Estévez, Ramos-Pineda, & Escribano-Bailón, 2018). With the purpose of studying the interactions between the different CWM obtained in this work and a soluble flavan-3-ol extract from grape seeds (F), ITC experiments were performed. ITC is one of the most useful techniques to characterize the binding reactions that take place between ligands and macromolecules, since it allows to understand the full thermodynamic picture of biomolecular interactions (Duff, Grubbs, & Howell, 2011; Ladbury, 2010).

In each interaction system (F-PSW1, F-PSW2, F-PSR1, and F-PSR2), two sets of sites (set1 and set2) were selected as independent sites to observe the values of thermodynamic parameters, including Gibbs free energy change (ΔG), apparent binding constant (K), and changes in enthalpy (ΔH) and in entropy (ΔS). It is important to highlight that ΔG values were negative for all systems, indicating that all CWM–flavan-3-ol interactions occurred spontaneously (Table 2). However, significant differences ($p < 0.05$) were found between the polysaccharide extracts. F-PSR1 and F-PSR2 bindings showed more negative ΔG scores (–2.218 $\times 10^4$ and –2.059 $\times 10^4$ cal mol^{-1}, respectively) than F-PSW1 and F-PSW2 interactions (–1.102 × 104 and –1.525 × 104 cal mol^{-1}), pointing out that soluble polysaccharides from red grapes interacted more spontaneously with the flavan-3-ols than the white ones. Considering the extraction phase, the white polysaccharides obtained in the first extraction showed lower absolute ΔG value (–1.102 $\times 10^4$ cal mol^{-1}) than those extracted within the second boiling water (–1.525 $\times 10^4$ cal mol^{-1}). On the contrary, this relation between the Gibbs free energy and the extraction phase did not keep up for polysaccharides from red grapes (Table 2). Interestingly, the most spontaneous interaction happened with the biggest CWM, PSR1 (~195 kDa), followed in ΔG intensity and size by PSR2 (~165 kDa), PSW2 (~141 kDa) and, finally, by PSW1 (~125 kDa). Hence, the mMW data allow us to establish an order of size (PSR1 > PSR2 > PSW2 > PSW1) that is in agreement with that found in the absolute ΔG scores, suggesting that, the mMW of soluble CWM might be one of the relevant factors for defining its interaction with the flavan-3-ols and that, in the range of kDa studied, the interaction between the flavan-3-ol extract and the soluble CWM is more favored as the mMW of the polysaccharide increases.

Table 2
Thermodynamic parameters for the CWM–flavan-3-ol interactions.

	F-PSW1	F-PSW2	F-PSR1	F-PSR2
ΔG_{total} (cal mol^{-1})	(-1.102 ± 0.007) × 10$^{4\ a}$	(-1.53 ± 0.01) × 10^{4b}	(-2.218 ± 0.004) × 10$^{4\ d}$	(-2.06 ± 0.03) × 10^{4c}
Set1				
K_1 (M^{-1})	(4.1 ± 0.5) × 10^{4c}	(3 ± 0.4) × 10^{6c}	(3.4 ± 0.4) × 10$^{8\ a}$	(1.52 ± 0.03) × 10^{8b}
ΔH_1 (cal mol^{-1})	(-6.2 ± 0.3) × 10$^{2\ a}$	(-8.0 ± 0.7) × 10$^{2\ a,b}$	(-1.7 ± 0.3) × 10$^{3\ d}$	(-1.2 ± 0.3) × 10^{3c}
$-T\Delta S_1$ (cal mol^{-1})	(-5.67 ± 0.07) × 10$^{3\ a}$	(-8.0 ± 0.1) × 10^{3b}	(-10.0 ± 0.4) × 10^{3c}	(-10 ± 0.3) × 10^{3c}
Set2				
K_2 (M^{-1})	(2.95 ± 0.09) × 10^{3c}	(5.3 ± 0.8) × 10^{4c}	(5.5 ± 0.5) × 10$^{7\ a}$	(8.3 ± 0.6) × 10^{6b}
ΔH_2 (cal mol^{-1})	(-6.7 ± 0.6) × 10^{2b}	(-7.6 ± 0.5) × 10^{2b}	(-2.9 ± 0.5) × 10$^{2\ a}$	(-7.3 ± 0.8) × 10^{2b}
$-T\Delta S_2$ (cal mol^{-1})	(-4.06 ± 0.07) × 10$^{3\ a}$	(-5.69 ± 0.04) × 10^{3b}	(-1.026 ± 0.002) × 10$^{4\ d}$	(-8.711 ± 0.005) × 10^{3c}

F: seed flavan-3-ols extract; PSW1: polysaccharides from white grapes (1st extraction); PSW2: polysaccharides from white grapes (2nd extraction); PSR1: polysaccharides from red grapes (1st extraction); and PSR2: polysaccharides from red grapes (2nd extraction). Different letters within the same row indicate statistical differences ($p < 0.05$, $n = 3$).

Additionally, thermodynamic parameters provide insights into the driving forces that govern the interaction processes: hydrophobic interactions (entropy-driven: $\Delta H > 0$, $-T\Delta S < 0$), hydrogen bonds (enthalpy-driven: $\Delta H < 0$, $-T\Delta S > 0$) or both types of forces if ΔH and $-T\Delta S$ are negative ($\Delta H < 0$, $-T\Delta S < 0$) (McRae, Falconer, & Kennedy, 2010). It was already described that the main forces implicated in the tannin–carbohydrate interactions are both hydrophobic interactions and H-bonds (Renard, Watrelot, & Le Bourvellec, 2017; Watrelot, Le Bourvellec, Imberty, & Renard, 2013; Bindon et al., 2010). Although the dominance of one of these forces depends on factors such as the specific composition and the flexible structure of the interacting compounds (Brandão et al., 2020; Watrelot, Le Bourvellec, Imberty, & Renard, 2014; Mateus, Carvalho, Luís, & De Freitas, 2004). Herein, the negative ΔH and $-T\Delta S$ scores for the two sets, in all systems (Table 2), reinforce the concurrency scenario. It has been reported that neutral side chains of pectic polysaccharides, which are mainly composed by residues of Ara and Gal, could favor the hydrophobic interactions with procyanidins whereas the cooperative H-bonds mainly take place between the oxygen atoms of polysaccharide uronic acids and the phenolic hydroxyl group (Brandão et al., 2020; Mateus et al., 2004).

Finally, the association constant values were higher for the F-PSR1 and F-PSR2 systems (3.437 $\times 10^8$ M^{-1} and 1.517 $\times 10^8$ M^{-1}, respectively in set1, and 5.470 $\times 10^7$ M^{-1} and 8.330 $\times 10^6$ M^{-1}, respectively in set2) (Table 2), highlighting again that red grapes CWM had a higher affinity to bind flavan-3-ols than the white ones. Altogether, the ITC data confirm the existence of interactions between flavan-3-ols and soluble CWM from grape skins and that the magnitude of the interaction depends on the polysaccharide structure and characteristics.

3.3. Effects of CWM addition on wine astringency and color

To determine the consequences of the CWM–flavan-3-ol interactions, evidenced by ITC, on wine astringency and color, 50 mg/L of PSW1, PSW2, PSR1 and PSR2 were added to four aliquots of a red wine previously treated with a freeze-dried soluble extract of seed flavan-3-ols (750 mg/L) to increase its astringency (Manjón et al., 2020; Alcalde-

Eon, Pérez-Mestre, et al., 2019).

An aliquot of this wine was labeled as control wine (C). Samples were conducted in triplicate and astringency and color were analyzed after one-week (1 W), three-week (3 W) and two-month (2 M) of storage at 22 °C.

Table 3 shows the results of the astringency evaluation. During all period of storage (1 W, 3 W, 2 M), PSW-wines (PSW1-wine and PSW2-wine) did not exhibit statistically different astringency intensities compared to the control, whereas PSR-wines (PSR1-wine and PSR2-wine) had statistically lower astringency intensities (decrease of >50 % after two months of storage) compared with the astringency of C, which suggests that red grape soluble CWM could be successfully used as wine astringency modulator.

To determine whether the addition of the soluble CWM leads to color changes in the wines, the color differences (ΔE^*_{ab}) between the control wine and the wine samples added with PSW1, PSW2, PSR1 and PSR2 during all period of storage (1 W, 3 W, 2 M) were studied (Table S3 of the Supplementary Material). It has been stablished that human eye is only able to detect color differences when ΔE^*_{ab} is higher than 3 (Martínez, Melgosa, Pérez, Hita, & Negueruela, 2001). As can be observed in Table S3 of the Supplementary Material, the color differences in the wine samples due to the addition of the soluble CWM were not visually perceptible except in case of wine analyzed two months after the addition of PSR2 where ΔE^*_{ab} was 3.22. The relative contribution of each color attribute that makes a given color difference value (ΔE^*_{ab}) was calculated as the quadratic differences of lightness, chroma, and hue (%Δ^2L, %Δ^2C, and %Δ^2H), employing the obtained colorimetric parameters (L^*, a^*, b^*, C^*_{ab}, h_{ab}) (Table S4 of the Supplementary Material) and the equations described by Gordillo and coworkers (Gordillo et al., 2015). The data indicated that the observed changes in color in PSR2-wine were mainly due to changes in lightness (%Δ^2L = 94.86 %), with little influence from chroma (%Δ^2C = 5.13 %) and hardly any variation in hue (%Δ^2H = 0.01 %). According to this, as can be observed in the Table S4 of the Supplementary Material, the wine supplemented during two months with PSR2 showed values of lightness significantly ($p < 0.05$) higher (52.5 ± 0.7) than the control (49.4 ± 0.4).

Therefore, no changes in astringency or wine color were observed by the addition of soluble CWM obtained from white grapes. On the contrary, the addition of soluble CWM obtained from red grapes allowed a significant decrease in the intensity of astringency perceived without modifying the color of the wine in case of PSR1 and, modifying slightly the lightness of the wine supplemented with PSR2 after storage. It has been previously observed that the addition of other types of polysaccharides to the wine, *i.e.* some mannoproteins, causes modification in CIELAB parameters that are visible to the human eye (Alcalde-Eon, García-Estévez, Puente, et al. (2014)). In fact, some mannoproteins intended for modulating astringency can have important negative effects on the coloring matter of wines (Alcalde-Eon, Pérez-Mestre, et al., 2019). This is not the case of PSR1 and PSR2, which could be proposed as a good option to be used when it is convenient to decrease the astringency but no modification of the wine color is intended.

To figure out if the decrease in astringency sensation is related to changes in the flavan-3-ol profile of the wines, the flavan-3-ol composition of wines was determined by means of HPLC-DAD-MS. Likewise, to rule out important changes in the anthocyanin profiles, the pigment composition was also analyzed.

Table 3
Astringency intensity of samples during storage.

Time	C-wine	PSW1-wine	PSW2-wine	PSR1-wine	PSR2-wine
1 W	8.8 ± 1.6 ^{a}	6.9 ± 2.7 ^{a,b}	6.7 ± 2.7 ^{a,b}	4.9 ± 2.1^{b}	4.7 ± 2.4^{b}
3 W	7.7 ± 1.5 ^{a}	9.3 ± 1.5 ^{a}	6.9 ± 2.9 ^{a,b}	4.7 ± 1.7^{b}	4.4 ± 2.1^{b}
2 M	7.1 ± 2.6 ^{a}	8.8 ± 1.3 ^{a}	7.9 ± 1.6 ^{a}	3.0 ± 0.9^{b}	3.4 ± 2.6^{b}

C: control wine; PSW1-wine: wine added with polysaccharides from white grapes (1st extraction); PSW2-wine: wine added with polysaccharides from white grapes (2nd extraction); PSR1-wine: wine added with polysaccharides from red grapes (1st extraction); and PSR2-wine: wine added with polysaccharides from red grapes (2nd extraction). Different letters within the same storage period indicate significant differences ($p < 0.05$, n = 8).

3.4. Effects of CWM addition on the Flavan-3-ol and anthocyanin profile

According to flavan-3-ol profile, 45 compounds were determined in the wine samples including 6 monomers, 15 dimers, 18 trimers and 6 tetramers (Table S5 of the Supplementary Material). For discussion, flavan-3-ols were grouped according to their structures, namely, non-galloylated monomeric flavan-3-ols (NGMF, 4 compounds), galloylated monomeric flavan-3-ols (GMF, 2 compounds), dimeric prodelphinidins (DPD, 2 compounds), dimeric procyanidins (DPC, 5 compounds), oligomeric procyanidins (OPC, 11 compounds), procyanidin-prodelphinidin mixed oligomers (OM, 21 compounds).

Fig. 1 shows the percentage of each flavan-3-ol group over the content in the wine control after two months of storage. The addition of soluble CWM obtained from red grapes (PSR1 and PSR2) resulted in a significant decrease ($p < 0.05$) in the content of total flavan-3-ols respecting to the control wine (30 % and 45 %, respectively), which is mainly due to a decrease in dimers and in oligomers of proanthocyanidins (Fig. 1). As stated in the ITC analysis, CWM could interact with flavan-3-ols via hydrogen bonds and hydrophobic interactions (Table 2). Thus, our data indicate that the interaction with red grape CWM leads to polysaccharide-flavan-3-ol complexes that could finally precipitate. As previously mentioned (Table 1), we found that CWM from red grapes contained higher proportions of AG, lower proportions of ARA and larger mMW than their white grape counterparts. Both AG and ARA are characterized as side chains in pectic polysaccharides: the AG regions confer pectins a more compact conformation, which can benefit the hydrophobic interaction (Alba, Bingham, & Kontogiorgos, 2017) meanwhile, ARA chains can limit the flavan-3-ol–polysaccharide interaction due to their highly branched structures (Watrelot et al., 2014; Watrelot et al., 2013). Therefore, red grape CWM may interact more effectively with flavan-3-ols than white grape CWM due to their compositional differences. Besides, the largest mMW of CWM from red grapes suggests that these CWM might bind more flavan-3-ols than their white grape counterparts due to a spatial advantage. Thus, although CWM from both white and red grape skins is able to interact with flavan-3-ols, CWM from red grapes might be capable of forming large polysaccharide–flavan-3-ol complexes that tend to precipitate leading to a flavan-3-ol loss.

It has been stated that the astringency threshold decreases from monomeric to dimeric and trimeric flavan-3-ols (García-Estévez et al.,

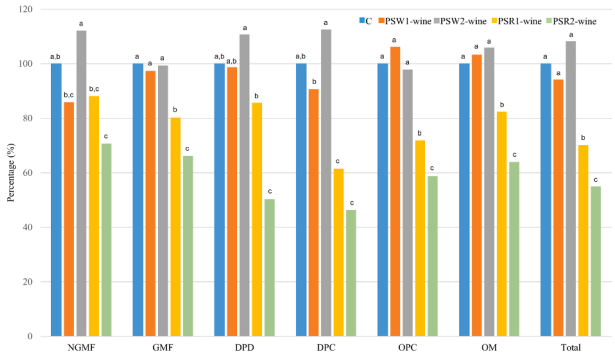

Fig. 1. Relative percentage of flavan-3-ols in comparison to the control after two months of storage. NGMF: non-galloylated monomeric flavan-3-ols; GMF: galloylated monomeric flavan-3-ols; DPD: dimeric prodelphinidins; DPC: dimeric procyanidins; OPC: oligomeric procyanidins (trimeric and tetrameric procyanidins); OM: mixed oligomers of (*epi*)catechin and (*epi*)gallocatechin. Different letters within each flavan-3-ol family indicate significant differences ($p < 0.05$, n = 3).

2018). These compounds can act as polydentate ligands binding salivary proteins and provoking its precipitation (De Freitas & Mateus, 2002) which in turn is the main mechanism that explains the astringent mouth feel. Therefore, some authors propose that the more polymerized the flavan-3-ols are, the more binding sites are available and consequently, greater is the astringency they could elicit, although steric hindrance should also be considered (García-Estévez et al., 2018). On this sense, the reduction in the content of dimers and oligomers of proanthocyanidins may be linked to the reduction of the astringency observed in our study.

As for anthocyanins, 28 compounds were determined (Table S6 of the Supplementary Material). For comparative purposes, pigments were grouped according to their structures in non-acylated monoglucosides (NAMO, 5 compounds), acylated monoglucosides (AMO, 11 compounds), flavan-3-ol-anthocyanin direct condensation products (FA, 1 compound), flavan-3-ol-anthocyanin acetaldehyde-mediated condensation products (FeA, 4 compounds), A-type vitisins (VitA, 1 compound), B-type vitisins (VitB, 2 compounds), and vinylphenol-type pyranoanthocyanins (VitVF, 4 compounds).

The Table 4 and Table S7 show the concentration of each anthocyanin group (mg/L), and total anthocyanins during storage. Slight differences in the content of pigments over the control wine were observed. Two months after storage higher total pigment content in the wines added with soluble CWM than in the control wine was determined (Table 4). This points to a certain protective effect of soluble CWM on anthocyanin pigments. Nevertheless, these differences do not provoke changes in color grater enough to be perceived (see Table S3 of the Supplementary Material).

The influence of soluble CWM addition on wine anthocyanins is very different from that caused by insoluble CWM addition, which is generally characterized by an anthocyanin loss (especially of monomeric anthocyanins) (Jiménez-Martínez et al., 2019; Guerrero et al., 2013). According to previous research, the main reason that caused anthocyanin loss after insoluble CWM addition should be the porous structure of insoluble CWM, which allowed anthocyanin molecules to penetrate in and then to be eliminated with the insoluble CWM by decanting or filtering (Guerrero et al., 2013; Bindon et al., 2010; Bautista-Ortín et al., 2016). Compared with the use of insoluble fibers or purified grape pomace, soluble CWM from red grapes has a better potential for astringency modulation, since no deleterious effects on color have not been observed.

Table 4
Concentration (mg/L) of anthocyanins* in samples after two months of storage.

2 months of storage					
Anthocyanin group	C-wine	PSW1-wine	PSW2-wine	PSR1-wine	PSR2-wine
NAMO	32.6 ± 0.6^{c}	36.2 ± 0.5 ^{a}	34.8 ± 0.9 ^{a,b}	34.0 ± 0.7^{c,b}	34.5 ± 0.7 ^{a,b}
AMO	21.9 ± 0.2^{b}	24 ± 1 ^{a}	24 ± 1 ^{a}	23.8 ± 0.5 ^{a}	23.1 ± 0.1 ^{a,b}
FA	2.2 ± 0.1 ^{a}	2.3 ± 0.2 ^{a}	2.2 ± 0.2 ^{a}	2.21 ± 0.05 ^{a}	2.2 ± 0.2 ^{a}
FeA	12.0 ± 0.6 ^{a}	12.6 ± 0.4 ^{a}	12.6 ± 0.4 ^{a}	13.0 ± 0.3 ^{a}	12.3 ± 0.8 ^{a}
VitA	3.3 ± 0.3 ^{a}	3.5 ± 0.3 ^{a}	3.3 ± 0.2 ^{a}	3.3 ± 0.2 ^{a}	3.3 ± 0.2 ^{a}
VitB	4.8 ± 0.3 ^{a}	4.5 ± 0.3 ^{a}	4.6 ± 0.6 ^{a}	4.4 ± 0.1 ^{a}	4.5 ± 0.3 ^{a}
VitVF	5.4 ± 0.2^{c}	6.1 ± 0.1 ^{a}	5.6 ± 0.3^{b,c}	5.94 ± 0.03 ^{a,b}	5.5 ± 0.3^{b,c}
Total	82.2 ± 0.9^{b}	90 ± 2 ^{a}	87 ± 3 ^{a,b}	87 ± 1 ^{a,b}	85 ± 2 ^{a,b}

*Expressed as malvidin 3-*O*-glucoside equivalents. NAMO: non-acylated monoglucosides of anthocyanins; AMO: acylated monoglucosides of anthocyanins; FA: flavan-3-ol-anthocyanin direct condensation products; FeA: flavan-3-ol-anthocyanin acetaldehyde-mediated condensation products; VitA: A-type vitisins; VitB: B-type vitisins; VitVF: vinylphenol type pyranoanthocyanins. Different letters within the same row indicate indicate significant differences ($p < 0.05$, $n = 3$).

3.5. Principal component analysis (PCA)

PCA was conducted as unsupervised pattern recognition to find out the relationships between wine astringency intensity (Ast), wine flavan-3-ol composition (NGMF, GMF, DPD, DPC, OPC, OM), and CWM composition (mMW, HG, RG I, RG II, AG, ARA, XG, MAN) after 2-months of storage. The first principal component (PC1) describes 59.3 % of the data variability whereas the second principal component (PC2) describes 22.1 %. Wines added with the CWM obtained from the same grape source are grouped together regardless of the first and second extraction, PSR-wines are separated from C and PSW-wines and are positively correlated with PC1 (Fig. 2A), in which AG is the main contributor.

Similar effects on wine flavan-3-ols and astringency were obtained in wines added with soluble CWM from the same grape skin source, regardless of their first or second extraction. As commented before, red grape CWM had statistically higher AG percentage and lower ARA percentage than those from white grapes (Table 1). Besides, soluble CWM from white grapes provides more small-molecular-weight macromolecules than their counterparts from red grapes.

As it can be observed in Fig. 2B, wine astringency shows a positive relationship with wine flavan-3-ols (especially oligomeric flavan-3-ols) but displays an opposition with polysaccharides except for ARA. As neutral sugar polysaccharides from side chains, ARA was reported to behave ineffectively during the interaction with flavan-3-ols due to its highly branched structures, which can limit their association with flavan-3-ols (Le Bourvellec & Renard, 2012; Watrelot et al., 2014). Therefore, polysaccharide extracts with high ARA rate might be inadvisable for decrease wine astringency. AG and mMW showed the biggest opposition to wine astringency and flavan-3-ols. The role of AG and AGP in affecting wine astringency is complex, depending on the detailed sugar composition, because acidic AGP can effectively decrease wine astringency, whereas neutral AGP promotes the aggregation between flavan-3-ols and salivary proteins, which could contribute to an increased astringency (Carvalho et al., 2006). In our study, red grape CWM contained higher proportion of AG than white grape CWM and the ratio between AG and ARA in white grape CWM was nearly 1; while it was 12 and 5 for the first and second extraction from red grape CWM, respectively. However, further molecular studies using isolated polysaccharides should be performed to assess the actual relevance of AG: ARA ratio.

Other grape CWM components (HG, RG I, RG II, XG, MAN) were also reported to show ability to interact with flavan-3-ols (Le Bourvellec & Renard, 2012; Bindon et al., 2012; Watrelot et al., 2014; Watrelot et al., 2013) but in our study these components did not show important differences related to the grape source and, therefore, they should not be responsible for explaining the different behavior observed between white and red grape CWM.

4. Conclusions

Here, for the first time, soluble CWM from red grape skins showed the ability to interact with wine flavan-3-ols reducing significantly the wine astringency (*ca.* 40 %), while soluble white grape CWM does not show important effects on wine astringency or wine color. Likewise, this study has allowed to stablish that the different effects between white and red CWM are related to their compositional differences, namely, red grape CWM contained more arabinogalactan (AG) and large-molecular-weight macromolecules, but less arabinan (ARA) than white grape CWM. Compared with the use of insoluble fibers or purified grape pomace, soluble CWM from different grapes did not result in significant loss in wine anthocyanins and color. Therefore, soluble CWM from red grapes has a good potential to be considered for astringency modulation

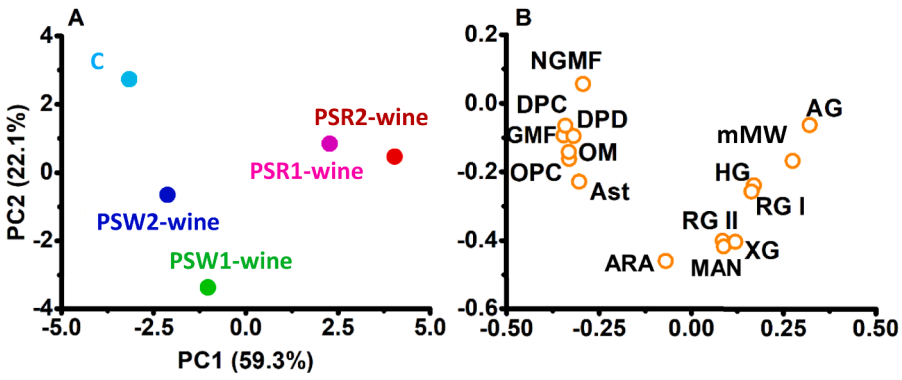

Fig. 2. Score plot (A) and loading plot (B) defined by the first and second principal components obtained in the principal component analysis for wines after two months of storage. mMW: medium molecular weight of soluble grape skin cell wall materials; HG: homogalacturonan; RG I: rhamnogalacturonan I; RG II: rhamnogalacturonan II; AG: arabinogalactan; ARA: arabinan; XG: xyloglucan; MAN: mannan. NGMF: non-galloylated monomeric flavan-3-ols; GMF: galloylated monomeric flavan-3-ols; DPD: dimeric prodelphinidins; DPC: dimeric procyanidins; OPC: oligomeric procyanidins (trimeric and tetrameric procyanidins); OM: mixed oligomers of (*epi*)catechin and (*epi*)gallocatechin; Ast: astringency intensity.

purposes. Thanks to this novel research, the possibility of obtaining useful polysaccharides from red grape skins arises, which could promote its valorization as by-product, favoring a more sustainable oenological process and contributing to the circular economy.

CRediT authorship contribution statement

Elvira Manjón: Conceptualization, Methodology, Investigation, Formal analysis, Writing – original draft, Visualization. **Siyu Li:** Conceptualization, Methodology, Investigation, Formal analysis, Writing – original draft, Visualization. **Montserrat Dueñas:** Conceptualization, Methodology, Investigation, Writing – original draft. **Ignacio García-Estévez:** Conceptualization, Methodology, Formal analysis, Supervision, Writing – review & editing, Project administration. **María Teresa Escribano-Bailón:** Conceptualization, Methodology, Supervision, Writing – review & editing, Project administration, Funding acquisition.

Declaration of Competing Interest

The authors declare that they have no known competing financial interests or personal relationships that could have appeared to influence the work reported in this paper.

Data availability

The data that has been used is confidential.

Acknowledgements

This work was supported by the Spanish Ministerio de Ciencia e Innovación (Project PID2021-127126OB-C21). Thanks are also due to Junta de Castilla y León-FEDER Programme for the Strategic Research Programs for Units of Excellence (Spain) (Project Ref. CLU-2O18-04). E. Manjón thanks Junta de Castilla y León-FEDER Programme (Project Ref. SA0093P20) for her postdoctoral contract. S. Li thanks the International Postdoctoral Exchange Fellowship Program 2018 by the Office of China Postdoctoral Council (No.39 Document of OCPC, 2018).

Appendix A. Supplementary data

Supplementary data to this article can be found online at https://doi.org/10.1016/j.foodchem.2022.134110.

References

Alba, K., Bingham, R. J., & Kontogiorgos, V. (2017). Mesoscopic structure of pectin in solution. *Biopolymers, 107*(6), e23016. https://doi.org/10.1002/bip.23016

Alcalde-Eón, C., Escribano-Bailón, M. T., Santos-Buelga, C., & Rivas-Gonzalo, J. C. (2006). Changes in the detailed pigment composition of red wine during maturity and ageing. A comprehensive study. *Analytica Chimica Acta, 563*(1–2), 238–254. https://doi.org/10.1016/j.aca.2005.11.028

Alcalde-Eon, C., García-Estévez, I., Ferreras-Charro, R., Rivas-Gonzalo, J. C., Ferrer-Gallego, R., & Escribano-Bailón, M. T. (2014). Adding oenological tannin vs. overripe grapes: Effect on the phenolic composition of red wines. *Journal of Food Composition and Analysis, 34*, 99–113. https://doi.org/10.1016/j.jfca.2014.01.004

Alcalde-Eon, C., García-Estévez, I., Puente, V., Rivas-Gonzalo, J. C., & Escribano-Bailón, M. T. (2014). Color stabilization of red wines. A chemical and colloidal approach. *Journal of Agricultural and Food Chemistry, 62*, 6984–6994. https://doi.org/10.1021/jf4055825

Alcalde-Eon, C., Ferreras-Charro, R., Ferrer-Gallego, R., Rivero, F. J., Heredia, F. J., & Escribano-Bailón, M. T. (2019). Monitoring the effects and side-effects on wine colour and flavonoid composition of the combined post-fermentative additions of seeds and mannoproteins. *Food Research International, 126*. https://doi.org/10.1016/j.foodres.2019.108650

Alcalde-Eon, C., Pérez-Mestre, C., Ferreras-Charro, R., Rivero, F. J., Heredia, F. J., & Escribano-Bailón, M. T. (2019). Addition of mannoproteins and/or seeds during winemaking and their effects on pigment composition and color stability. *Journal of Agricultural and Food Chemistry, 67*(14), 4031–4042. https://doi.org/10.1021/acs.jafc.8b06922

Arnous, A., & Meyer, A. S. (2009). Quantitative prediction of cell wall polysaccharide composition in grape (*Vitis vinifera* L.) and apple (*Malus domestica*) skins from acid hydrolysis monosaccharide profiles. *Journal of Agricultural and Food Chemistry, 57*(9), 3611–3619. https://doi.org/10.1021/jf900780r

Bautista-Ortín, A. B., Martínez-Hernández, A., Ruiz-García, Y., Gil-Muñoz, R., & Gómez-Plaza, E. (2016). Anthocyanins influence tannin-cell wall interactions. *Food Chemistry, 206*, 239–248. https://doi.org/10.1016/j.foodchem.2016.03.045

Bindon, K. A., Smith, P. A., & Kennedy, J. A. (2010). Interaction between grape-derived proanthocyanidins and cell wall material. 1. Effect on proanthocyanidin composition and molecular mass. *Journal of Agricultural and Food Chemistry, 58*(4), 2520–2528. https://doi.org/10.1021/jf9037453

Bindon, K. A., Bacic, A., & Kennedy, J. A. (2012). Tissue-specific and developmental modifications of grape cell walls influence the adsorption of proanthocyanidins. *Journal of Agricultural and Food Chemistry, 60*(36), 9249–9260. https://doi.org/10.1021/jf301552t

Brandão, E., Fernandes, A., Guerreiro, C., Coimbra, M. A., Mateus, N., de Freitas, V., & Soares, S. (2020). The effect of pectic polysaccharides from grape skins on salivary protein–procyanidin interactions. *Carbohydrate Polymers, 236*, Article 116044. https://doi.org/10.1016/j.carbpol.2020.116044

Carvalho, E., Mateus, N., Plet, B., Pianet, I., Dufourc, E., & De Freitas, V. (2006). Influence of wine pectic polysaccharides on the interactions between condensed tannins and salivary proteins. *Journal of Agricultural and Food Chemistry, 54*(23), 8936–8944. https://doi.org/10.1021/jf061835h

De Freitas, V., & Mateus, N. (2002). Nephelometric study of salivary protein-tannin aggregates. *Journal of the Science of Food and Agriculture, 82*(1), 113–119. https://doi.org/10.1002/jsfa.1016

Duff, M. R., Grubbs, J., & Howell, E. E. (2011). Isothermal titration calorimetry for measuring macromolecule-ligand affinity. *Journal of Visualized Experiments, 55*, 1–4. https://doi.org/10.3791/2796

Ferrer-Gallego, R., Quijada-Morín, N., Brás, N. F., Gomes, P., de Freitas, V., Rivas-Gonzalo, J. C., & Escribano-Bailón, M. T. (2015). Characterization of sensory properties of flavanols-A molecular dynamic approach. *Chemical Senses, 40*(6), 381–390. https://doi.org/10.1093/chemse/bjv018

Ferrer-Gallego, R., Brás, N. F., García-Estévez, I., Mateus, N., Rivas-Gonzalo, J. C., De Freitas, V., & Escribano-Bailón, M. T. (2016). Effect of flavonols on wine astringency and their interaction with human saliva. *Food Chemistry, 209*, 358–364. https://doi.org/10.1016/j.foodchem.2016.04.091

García-Estévez, I., Alcalde-Eon, C., & Escribano-Bailón, M. T. (2017). Flavanol quantification of grapes via multiple reaction monitoring mass spectrometry. Application to differentiation among clones of *Vitis vinifera* L. cv. Rufete grapes. *Journal of Agricultural and Food Chemistry, 65*, 6359–6368. https://doi.org/10.1021/acs.jafc.6b05278

García-Estévez, I., Ramos-Pineda, A. M., & Escribano-Bailón, M. T. (2018). Interactions between wine phenolic compounds and human saliva in astringency perception. *Food and Function, 9*(3), 1294–1309. https://doi.org/10.1039/c7fo02030a

Gordillo, B., Rodríguez-Pulido, F. J., Escudero-Gilete, M. L., Gonzalez-Miret, M. L., & Heredia, F. J. (2012). Comprehensive colorimetric study of anthocyanic copigmentation in model solutions. Effects of pH and molar ratio. *Journal of Agricultural and Food Chemistry, 60*(11), 2896–2905. https://doi.org/10.1021/jf2046202

Gordillo, B., Rodríguez-Pulido, F. J., González-Miret, M. L., Quijada-Morín, N., Rivas-Gonzalo, J. C., García-Estévez, I., … Escribano-Bailón, M. T. (2015). Application of differential colorimetry to evaluate anthocyanin-flavonol-flavanol ternary copigmentation interactions in model solutions. *Journal of Agricultural and Food Chemistry, 63*(35), 7645–7653. https://doi.org/10.1021/acs.jafc.5b00181

Green, B. G., Dalton, P., Cowart, B., Shaffer, G., Rankin, K., & Higgins, J. (1996). Evaluating the "labeled magnitude scale" for measuring sensations of taste and smell. *Chemical Senses, 21*(3), 323–334. https://doi.org/10.1093/chemse/21.3.323

Guadalupe, Z., Martínez, L., & Ayestarán, B. (2010). Yeast mannoproteins in red winemaking: Effect on polysaccharide, polyphenolic, and color composition. *American Journal of Enology and Viticulture, 61*(2), 191–200.

Guerrero, R. F., Smith, P., & Bindon, K. A. (2013). Application of insoluble fibers in the fining of wine phenolics. *Journal of Agricultural and Food Chemistry, 61*(18), 4424–4432. https://doi.org/10.1021/jf400172f

Heredia, F.J.; Álvarez, C.; González-Miret, M. L.; Ramírez, A. (2004). *CromaLab, análisis de color; Registro General de la Propiedad Intelectual No. SE-1052-04e, Sevilla, Spain.*

Jiménez-Martínez, M. D., Bautista-Ortín, A. B., Gil-Muñoz, R., & Gómez-Plaza, E. (2019). Comparison of fining red wines with purified grape pomace versus commercial fining agents: Effect on wine chromatic characteristics and phenolic content. *International Journal of Food Science and Technology, 54*(4), 1018–1026. https://doi.org/10.1111/ijfs.13881

Jiménez-Martínez, M. D., Bautista-Ortín, A. B., Gil-Muñoz, R., & Gómez-Plaza, E. (2019). Fining with purified grape pomace. Effect of dose, contact time and varietal origin on the final wine phenolic composition. *Food Chemistry, 271*, 570–576. https://doi.org/10.1016/j.foodchem.2018.08.009

Jones-Moore, H. R., Jelley, R. E., Marangon, M., & Fedrizzi, B. (2022). The interactions of wine polysaccharides with aroma compounds, tannins, and proteins, and their importance to winemaking. *Food Hydrocolloids, 123*, Article 107150. https://doi.org/10.1016/j.foodhyd.2021.107150

Jones, G. V., White, M. A., Cooper, O. R., & Storchmann, K. (2005). Climate change and global wine quality. *Climatic Change, 73*(3), 319–343. https://doi.org/10.1007/s10584-005-4704-2

Ladbury, J. E. (2010). Calorimetry as a tool for understanding biomolecular interactions and an aid to drug design. *Biochemical Society Transactions, 38*(4), 888–893. https://doi.org/10.1042/BST0380888

Le Bourvellec, C., & Renard, C. M. G. C. (2012). Interactions between polyphenols and macromolecules: Quantification methods and mechanisms. *Critical Reviews in Food Science and Nutrition, 52*(3), 213–248. https://doi.org/10.1080/10408398.2010.499808

Martínez-Lapuente, L., Guadalupe, Z., and Ayestaran, B. (2019). Properties of Wine Polysaccharides. In *Pectins - Extraction, Purification, Characterization and Applications*, 1–21.

Manjón, E., Brás, N. F., García-Estévez, I., & Escribano-Bailón, M. T. (2020). Cell wall mannoproteins from yeast affect salivary protein-flavanol interactions through different molecular mechanisms. *Journal of Agricultural and Food Chemistry, 68*(47), 13459–13468. https://doi.org/10.1021/acs.jafc.9b08083

Martínez, J. A., Melgosa, M., Pérez, M. M., Hita, E., & Negueruela, A. I. (2001). Note. Visual and instrumental color evaluation in red wines. *Food Science and Technology International, 7*, 439–444. https://doi.org/10.1106/VFAT-5REN-1WK2-5JGQ

Martins, V. M. R., Simões, J., Ferreira, I., Cruz, M. T., Domingues, M. R., & Coimbra, M. A. (2017). In vitro macrophage nitric oxide production by *Pterospartum tridentatum* (L.) Willk. inflorescence polysaccharides. *Carbohydrate Polymers, 157*, 176–184. https://doi.org/10.1016/j.carbpol.2016.09.079

Mateus, N., Carvalho, E., Luís, C., & De Freitas, V. (2004). Influence of the tannin structure on the disruption effect of carbohydrates on protein-tannin aggregates. *Analytica Chimica Acta, 135–140*. https://doi.org/10.1016/j.aca.2003.08.072

McRae, J. M., Falconer, R. J., & Kennedy, J. A. (2010). Thermodynamics of grape and wine tannin interaction with polyproline: Implications for red wine astringency. *Journal of Agricultural and Food Chemistry, 58*(23), 12510–12518. https://doi.org/10.1021/jf1030967

Renard, C. M. G. C., Watrelot, A. A., & Le Bourvellec, C. (2017). Interactions between polyphenols and polysaccharides: Mechanisms and consequences in food processing and digestion. *Trends in Food Science and Technology, 60*, 43–51. https://doi.org/10.1016/j.tifs.2016.10.022

Scollary, G. R., Pásti, G., Kállay, M., Blackman, J., & Clark, A. C. (2012). Astringency response of red wines: Potential role of molecular assembly. *Trends in Food Science and Technology, 27*(1), 25–36. https://doi.org/10.1016/j.tifs.2012.05.002

Soares, S., Santos-Silva, M., García-Estévez, I., Brandão, E., Fonseca, F., Ferreira-da-Silva, F., … de Freitas, V. (2019). Effect of malvidin-3-glucoside and epicatechin interaction on their ability to interact with salivary proline-rich proteins. *Food Chemistry, 276*, 33–42. https://doi.org/10.1016/j.foodchem.2018.09.167

Watrelot, A. A., Le Bourvellec, C., Imberty, A., & Renard, C. M. G. C. (2013). Interactions between pectic compounds and procyanidins are influenced by methylation degree and chain length. *Biomacromolecules, 14*, 709–718. https://doi.org/10.1021/bm301796y

Watrelot, A. A., Le Bourvellec, C., Imberty, A., & Renard, C. M. G. C. (2014). Neutral sugar side chains of pectins limit interactions with procyanidins. *Carbohydrate Polymers, 99*, 527–536. https://doi.org/10.1016/j.carbpol.2013.08.094

Zhang, B., Gao, Y., Zhang, L., & Zhou, Y. (2021). The plant cell wall: Biosynthesis, construction, and functions. *Journal of Integrative Plant Biology, 63*(1), 251–272. https://doi.org/10.1111/jipb.13055

Zhang, Y., Zhang, P., Wang, Z., & Huang, L. (2011). An innovative derivatization method for simultaneous determination of uronic acids and neutral and amino sugars in coexisting samples by HPLC-ESI-MS/MS2. *Journal of Liquid Chromatography and Related Technologies, 34*, 1754–1771. https://doi.org/10.1080/10826076.2011.579216